Baltic Astronomy, vol.4, 402–412, 1995.

A 3-D SPH MODEL OF HELIUM ACCRETION DISKS IN THE INTERACTING BINARY WHITE DWARF SYSTEMS AM CVn AND EC 15330-1403

M. A. Wood and J. C. Simpson

Department of Physics and Space Sciences, Florida Institute of Technology, Melbourne, Florida 32901, U.S.A.

Received August 30, 1995.

Abstract. of the helium accretion disks in the interacting binary white dwarf systems AM CVn and EC 15330–1403. These systems are apparently in continuous high state, suggesting high mass transfer rates and an approximately steady state disk structure. Our results are consistent with this model in that we find that, if a large artificial viscosity is used, the simulation develops spiral shocks which are quasi-stationary in the corotating frame of reference. These $m = 2$ spiral patterns should give rise to photometric variations with $P = \frac{1}{2}P_{\rm orb}$, long inferred for AM CVn. Considerable departures from the average shock structure are seen on a timescale of a few orbits, but our results suggest that the point symmetry and phase of the shocks are maintained in the long term. The former is consistent with Fourier spectra which are variable for data runs of only a few hours in length, while the latter is consistent with long term stability of the light curve and absence of the fundamental frequency as found in WET observations. It has been suggested that a permanent superhump phenomenon explains the 20.77 μHz splitting observed in the time series photometry and the corresponding 13.38 h spectroscopic line-profile variations. We discuss our results within the context of this model.

Key words: hydrodynamics – methods: numerical – stars: binaries – stars: cataclysmic variables – stars: individual: AM CVn, EC 15330-1403

1. Introduction

The system AM CVn and its near twin EC 15330–1403 are interacting binary white dwarf (IBWD) cataclysmic variable systems, which as an observed class are characterized by their nearly pure helium spectra, their unusual spectral line profiles and their short-period photometric variations. The model generally favored for the IBWDs is that of a Roche-lobe-overflowing, low-mass ($M_2 \sim 0.05\ M_\odot$), weakly degenerate helium secondary which transfers mass onto the primary ($M_1 \sim 1.0\ M_\odot$) via an accretion disk (Faulkner, Flannery & Warner 1972). These systems, reviewed most recently by Warner (1995), are estimated to have $M_V \sim 9.5$ and number only 6 at present, indicating that they are rare objects ($\rho_{\rm IBWD} \sim 3\times10^{-6}$ pc^{-3}. Their orbital periods are inferred to be $P_{\rm orb} \lesssim 50$ min, and their corresponding orbital separations are $a \sim 0.25\ R_\odot$. Two of the systems, AM CVn and EC 15330–1403, are evidently in permanent outburst, similar to the nova-like variables. The optical spectrum of the system GP Com (=G 61–29) shows emission lines and no detected photometric variations – suggesting a system in quiescence with very low-mass transfer rate – and GP Com is the only IBWD to be also a spectroscopic binary with a firm orbital period determination ($P_{\rm orb} = 2970$ s). The remaining three objects, CR Boo (=PG 1346+082), V 803 Cen (=AE1) and CP Eri, all exhibit large-amplitude ($\Delta m \lesssim 4$ mag) photometric variations on a timescale of days, suggesting intermediate mass transfer rates and thermal instabilities in the disk arising from the ionization phase transition as discussed by Smak (1983).

The system AM CVn in particular has a long history in the literature, and a number of models have been proposed to explain the observed photometric and spectroscopic variations (see, for example, Patterson et al. 1992, 1993; Provencal et al. 1995). To date, however, few numerical explorations specific to these helium mass-transfer systems have been published – a situation we hope to remedy, beginning with this report. We have recently developed an efficient smoothed particle hydrodynamics (SPH) code (see Simpson 1995), in part to study in detail the dynamics of the AM CVn disks and to attempt to calculate their light curves. Here we present preliminary results for a purely hydrodynamic three-dimensional model of a helium disk in a system with a mass ratio of $q \equiv M_2/M_1 = 0.08$ (for a general review of SPH methods, see Monaghan 1992). In the following section, we discuss the numerics of the models, and in § 3 we dis-

cuss the results. Finally, in § 4 we compare our results with the recent numerical evidence for accretion precession as an explanation for the observed superhump phenomenon (Whitehurst 1988, 1994; Whitehurst & King 1991).

2. The numerical model and physical parameters

2.1. The numerics

A detailed description of the equations of motion and the numerical techniques are given by Simpson (1995). Briefly, the equations of motion are solved in an inertial frame of reference with the origin located at the center of mass of the two stars. Self-gravitation in the disk is not included. Disk particles are subject only to fluid forces (pressure and viscous) summed vectorially pairwise over "nearest neighbors," as well as the gravitational forces due to the two point masses M_1 and M_2, which are taken to be in circular orbits with respect to the center of mass. Radiative cooling is not included explicitly; instead, we use an ideal gas equation of state $p = (\gamma - 1)\rho u$ with a low adiabatic index of $\gamma = 1.01$.

The nearest neighbors of a given particle are those particles within two smoothing lengths h of the particle position, and the strength of the interaction between any two particles i and j is determined by a smoothing kernel $W(r_{ij})$. In the model presented here, the smoothing length is chosen to be 2 percent of the orbital separation, $h = 0.02a$, and the number of particles for the steady-state disk is maintained at $N = 6000$. This gives an average number of nearest neighbors $N_{\rm NN} \approx 30$.

The computations are made in dimensionless units where distances are measured in units of orbital separation a and masses in solar masses $M_\odot$. The unit of velocity is $[G(M_1 + M_2)/a]^{1/2}$ so that the orbital period becomes 2π using Kepler's law. The calculational space is defined by a rectangular box centered at the origin with sides $2a$ and z extent $0.48a$. All particles have equal mass and size, however, it is important to emphasize that the actual particle mass is *arbitrary* and has no effect on the dynamics of the disks within our assumptions, provided that the particles interact only with each other.

Each particle is injected into the system with a radial speed corresponding to the thermal speed of the secondary's atmosphere

and with the angular momentum appropriate to its randomly chosen position within a corotating cube of side $0.04a$ that has one face centered at the inner Lagrange point $\mathcal{L}_1$. The disk is built up by injecting 1000 particles per orbit for the first 6 orbits, and then is maintained at $N = 6000$ by replacing all particles that cross into the volumes of the primary or secondary or that are ejected from the system. There is no attempt to model any type of boundary conditions at the surface of either star: a particle crossing either star's surface or the limits of the system is simply removed from the calculation, and replaced by another with the same label but located within the injection box with the appropriate velocity and internal energy.

Particle trajectories are followed using the 2nd-order-accurate leapfrog method (see Hockney & Eastwood 1988) where the timestep used by an individual particle is determined dynamically and is allowed to take on discrete values ranging from $\Delta t_0 = P_{\rm orb}/100$ to a minimum value $\Delta t_{\rm min} = 2^{-(n-1)}\Delta t_0$, as needed, and where $n = 6$ was used to give an adequate resolution of the timescales from the orbit of the secondary to the "surface" of the primary white dwarf R_1.

Viscous interactions are introduced using a numerical viscosity Π that depends linearly on the product of the relative velocity difference and the average of the sound speeds of the two particles, converting some of the particles' kinetic energy into internal energy (i.e., heat) (Monaghan 1992):

$$\Pi_{ij} = -\alpha \bar{c}_{ij} \mu_{ij} / \bar{\rho}_{ij}, \tag{1}$$

where c is the sound speed, ρ is the density, and

$$\mu_{ij} = \frac{h \mathbf{v}_{ij} \cdot \mathbf{r}_{ij}}{r_{ij}^2 + \eta^2}. \tag{2}$$

The quantity α is a dimensionless constant of order unity that we set equal to 3, $\bar{\rho}_{ij} = \frac{1}{2}(\rho_i + \rho_j)$, and $\bar{c}_{ij} = \frac{1}{2}(c_i + c_j)$. The η^2 term is a constant and is used to prevent numerical divergences; we use $\eta^2 = 0.01h^2$.

We allow the artificial viscosity to act on both *approaching and receding* particles, contrary to the usual practice in SPH calculations of assuming that viscosity acts only on approaching particles (the particle analog of $\nabla \cdot \mathbf{v} < 0$). The suggestion to calculate viscous interactions for all particle pairs was originally made by Artymowicz &

Lubow (1994), motivated by the fact that the viscosity in the Navier-Stokes equation remains nonzero, in general, independent of whether the flow is converging or expanding. We find that this change results in to significantly more well-defined disks with higher accretion rates onto M_1. These disks also spread out more into the regions where the 3:1 orbital corotation resonance should excite eccentric modes. However, our use of this particular viscosity prescription is a recent change; consequently, our results are currently limited to 25 binary orbits.

2.2. The physical parameters

The following physical parameters are used to broadly represent the systems AM CVn and EC 15330–1403: mass of primary $M_1 = 1\ M_\odot$, mass of secondary $M_2 = 0.08\ M_\odot$, orbital period $P_{\rm orb} = 1100$ s and a pure helium atmosphere for the secondary with a temperature of $T_{M_2} = 2000$ K. The orbital separation a is determined using Kepler's third law so that $a = 0.2357\ R_\odot$ for this system. The radius of the primary is 5.6×10^8 cm, and the secondary M_2 is assumed to fill its Roche lobe. In order to obtain physical accretion rates, we set the particle mass at $m = 2 \times 10^{17}$ g, with a corresponding physical density of $\rho \approx 10^{-9}$ g cm^{-3}.

3. Results

The projections of all particles onto the orbital (x, y) plane at the end of selected orbits are shown in Fig. 1. Once the disk has stabilized after about 10 orbits, spiral shocks become evident which are variable in appearance over timescales of a few orbits, but whose average positions are fixed in the corotating frame. The spiral shocks should give rise to enhancements of the local surface brightness, and in an optically-thick disk with a concave photosphere viewed with an inclination $i \gtrsim 30°$, these bright regions should give rise to luminosity variations with a period of 1/2 the orbital period. To the extent that the spiral shocks move with respect to their average position, we would expect "phase jitter" in the resulting light curve, consistent with the time-series-photometric data from these systems (see Solheim et al. 1984, 1996, in preparation; Wood et al. 1987; Patterson et al. 1992). To the extent that the mean shock position is stable and point symmetric in the rotating frame, however, we would expect to find long-term phase and period stability in the ob-

served photometric variations, and would further expect that long data runs could show an absence of the orbital period in the Fourier transform, consistent with the recent analysis of the Whole Earth Telescope (WET) data from the system AM CVn (Provencal et al. 1995).

Our models do not yet include radiation losses directly, and so we are not able to compute a light curve for these systems at this time. We are, however, working in this direction and will have more to say in a future publication.

We find an $m = 1$ elongation of the disk in our results, but in the first 25 orbits we do not find convincing evidence for precession as inferred from observations of the variable spectral-line profiles (Patterson et al. 1993), or as found computationally by Whitehurst (1988, 1994), Whitehurst & King (1991) and Hirose & Osaki (1990). For comparison, note that Whitehurst (1994) found significant eccentric mode power only beyond orbit ~40. We are currently working to extend our simulations. Disk precession is thought to be responsible for the superhump (SH) phenomenon observed in the SU UMa cataclysmic variables, where the beat between the orbital period and the disk precession period gives rise to a photometric period longward of the orbital period, $P_{\rm SH} = P_{\rm orb} + \Delta P$, where ΔP is a function of mass ratio. It has been suggested that AM CVn may be a system in permanent superoutburst with an orbital period of 1029 s (Patterson et al. 1993; Warner 1995), analogous to the nova-like variable PG 0917+342 which has $P_{\rm orb} = 1.80$ h and a brightness modulation at $P = 1.88$ h. We will require a significantly longer simulation – of order 100 orbits – and ultimately a method for estimating the light curves from these systems before we can address these issues in any detail. For now, we can only note that our results are consistent with this model.

In Fig. 2 we show the particle positions in the (r, z) plane, effectively wrapping about the vertical axis to give a cross-sectional view of the disk. A pile-up of matter at the circularization radius is clearly visible. The disk is very thin with the disk semi-thickness $H \sim R^{\frac{9}{8}}$ in the inner regions as predicted by the α–disk model of Shakura & Sunyaev (1973). Increasing the number of particles N in the simulation and decreasing the smoothing length h further decreases the disk thickness.

A logarithmic plot of the internal energy (i.e., temperature) as a function of distance from M_1 is shown in Fig. 3. Cooler particles are seen entering the circularization region via the mass transfer

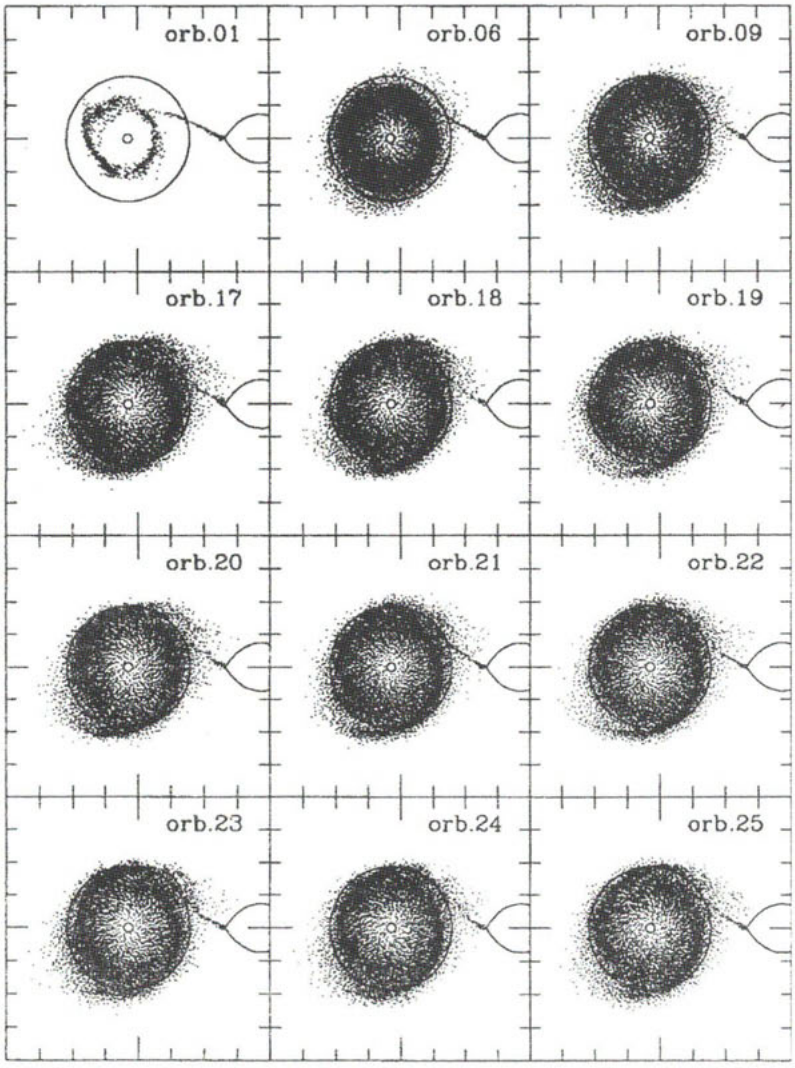

Fig. 1. The projections of all particles onto the orbital plane at the end of selected orbits. The radius of the primary is shown to scale, as is the tidally-distorted surface of the secondary near the $\mathcal{L}_1$ point. The large circle in each frame indicates the location of the 3:1 orbital corotation resonance. Note the variable nature of the spiral shocks about a mean position.

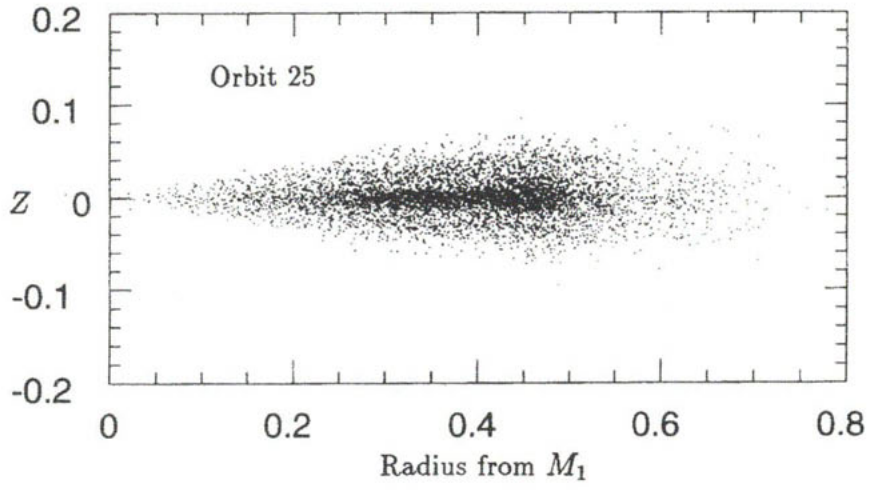

Fig. 2. Disk profiles of the disk height versus radial distance from M_1 at the end of orbit 25. Note the thin nature of the disk and the high density at the circularization radius.

stream. These particles then heat up until they move out of this region and are captured by either the primary or recaptured by the secondary. The inner disk regions are characterized by $T \sim R^{-1}$, which is comparable to the result $T \sim R^{-\frac{3}{4}}$ of Lanzafame, Belvedere & Molteni (1992), who use a polytropic equation of state but the same low adiabatic gamma.

If the internal units are converted back to physical units, the temperatures in the disk are found to range from $\sim 9 \times 10^5$ K to $\sim 4 \times 10^7$ K, which is about a factor of 10 larger than the values predicted by the α model and also those inferred from observations. In addition, the outer disk regions are much too hot. Both of these effects are presumably due to the lack of radiative cooling in the model. We are working to include radiative cooling into our SPH code, and will report on those results in a future publication.

The accretion rates in units of particles per binary orbit for both the primary and secondary are shown in Figure 4. It can be seen the rates onto M_1 reach equilibrium after $\approx$ 20 binary orbits, but that the rates for M_2 show large fluctuations. Because the mass of the particles does not affect the dynamics or thermal structure of the disk in our approximations, comparisons of our accretion rates with the observed rates are rather arbitrary. Using a particle mass

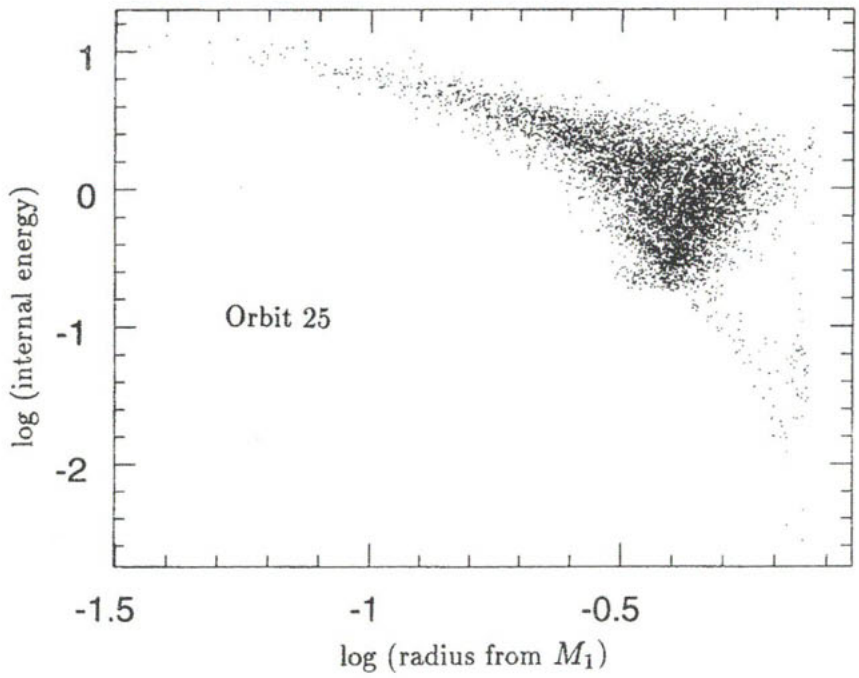

Fig. 3. The logarithm of the dimensionless internal energy as a function of distance from M_1.

of 2×10^{17} g, we obtain accretion rates of $\sim 10^{-9}\ M_\odot\ \mathrm{yr}^{-1}$ for this simulation — consistent with the rate inferred from the observations (see Warner 1995).

Comparing the mean replacement rate with the total number of particle in the disk, we find that a given particle will spend on average ~ 15 system orbits in the disk before being accreted by one of the stars. The fraction of injected particles that are accreted onto the secondary is about 20 %, comparable to the results obtained by Lin & Papaloizou (1979) for similar mass ratios. Less than 1 % of the transferred particles are scattered out of the system.

4. Conclusions

We have presented simulations of hydrodynamic helium accretion disks in a system with $q = 0.08$ and physical parameters chosen to represent the IBWD systems AM CVn and EC 15330–1403. Using

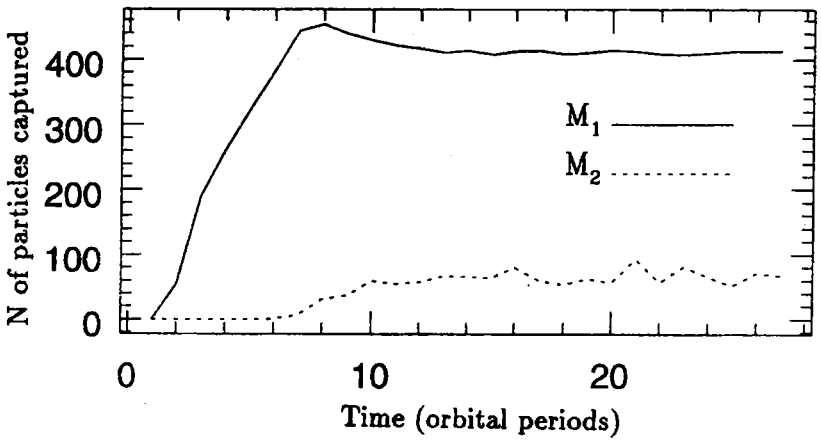

Fig. 4. Accretion rates onto M_1 and M_2 in units of particles per orbit.

a high artificial viscosity that acts on both approaching and receding particle pairs, our models rapidly develop spiral shocks which are only quasi-stationary in the corotating frame. We suggest that the variations in the shock position and strength would result in the observed "phase jitter" in these systems, but that long averages should produce a stable period. Our results are consistent with the model of a system in permanent superoutburst, similar to the SU UMa systems, although much more work is required to explore the fine details of the disk dynamics and expected light curves.

Finally, we note once again for emphasis that these are purely hydrodynamic disks, and are therefore incomplete models. Radiative cooling effects at a minimum must clearly be included for a more representative model, especially near the outer disk regions where our models are much too hot. Also, our results may be skewed by our use of constant-mass, constant-h particles, and we are planning to implement a particle merging/splitting routine to our models, similar to that used described in Meglicki, Wickramasinghe, & Bicknell (1993). We are working to improve the physics in our models.

Acknowledgments. This work was supported in part by NSF grant AST-9217988.

References

Artymowicz P., Lubow S.H. 1994, ApJ, 421, 651
Faulkner J., Flannery B., Warner B. 1972, ApJ, 175, L79
Hirose M., Osaki Y. 1990, PASJ, 42, 135
Hockney R.W., Eastwood J.W. 1988, Computer Simulations Using Particles, 2nd Ed., Institute of Physics Publishing, Bristol
Lanzafame G., Belvedere G., Molteni D. 1992, MNRAS, 258, 152
Lin D.N.C., Papaloizou J. 1979, MNRAS, 186, 799
Meglicki Z., Wickramasinghe D., Bicknell G. 1993, MNRAS, 264, 691
Monaghan J.J. 1992, ARA&A, 30, 543
Patterson J., Halpern J., Shambrook A. 1993, ApJ, 419, 803
Patterson J., Sterner E., Halpern J.P., Raymond J.C. 1992, ApJ, 384, 234
Provencal J.L. et al. 1995, ApJ, 445, 927
Shakura S.J., Sunyaev R.A. 1973, A&A, 24, 337
Simpson J.C. 1995, ApJ, 448, 822
Smak J. 1983 1994, Acta Astron., 33, 333
Solheim J.-E., Robinson E.L., Nather R.E., Kepler S.O. 1984, A&A, 135, 1.
Solheim J.-E. et al. 1996, Whole Earth Telescope Observations of AM CVn, in preparation.
Warner B., Ap&SS, 225, 249
Whitehurst R. 1994, MNRAS, 266, 35
Whitehurst R. 1988, MNRAS, 232, 35
Whitehurst R., King A. 1991, MNRAS, 249, 25
Wood M.A., Winget D.E., Nather R.E., Hessman F.V., Liebert J., Kurtz D.W., Wessemal F., Wegner G. 1987, ApJ, 313, 757